

# Multilayer Langmuir–Blodgett assemblies of hydrophobized CdS nanoparticles by organization at the air–water interface

Chinmay Damle, Anand Gole and Murali Sastry\*

Materials Chemistry Division, National Chemical Laboratory, Pune 411 008, India.  
E-mail: sastry@ems.ncl.res.in; Fax: +91-20-5893044/5893952; Tel: +91-20-5893044

Received 24th December 1999, Accepted 8th March 2000

Published on the Web 4th May 2000

The formation of multilayer Langmuir–Blodgett (LB) films of hydrophobized CdS nanoparticles by organization at the air–water interface is described. The hydrophobization of CdS nanoparticles (60 Å diameter) synthesized in an aqueous medium is accomplished by extraction of the particles from solution into thermally evaporated octadecylamine (ODA) films. Vigorous stirring of the ODA–CdS nanocomposite films in organic solvents resulted in dispersion of the CdS particles in the organic phase. The hydrophobic CdS nanoparticles were dispersed on the surface of water, organized into a fairly closely packed monolayer and multilayer films formed on different substrates by the versatile Langmuir–Blodgett technique. The organization of the particles and formation of multilayer films by the Langmuir–Blodgett technique was followed by surface pressure–area isotherm measurements of the nanoparticle Langmuir monolayer, quartz crystal microgravimetry, contact angle measurements, UV–vis spectroscopy and Fourier transform infrared spectroscopy studies. It is observed that a reasonably close-packed monolayer of the CdS nanoparticles forms on the surface of water and that excellent multilayer films of the particles can be grown on different supports *via* sequential transfer by the LB technique.

## Introduction

The unusual physicochemical and optoelectronic properties of nanoscale materials have stimulated much interest in this area.<sup>1</sup> Semiconductor nanoparticles in particular have been receiving much attention due to their potential applications in non-linear optics,<sup>2</sup> light emitting diodes<sup>3</sup> and quantum dot lasers.<sup>4</sup> In the quantum or so-called Q-state regime, the ability to vary the optical and electronic properties of a material through changing the size of the particle affords great flexibility in the band-gap engineering of materials.<sup>5</sup>

The organization and packaging of Q-state semiconductor particles, particularly as thin films, is an important problem *en route* to commercial exploitation of these nanoparticles. A number of techniques have been used to organize Q-state CdS nanoparticles in thin film form. Some of the important examples include chemical treatment of Langmuir monolayers<sup>6</sup> and Langmuir–Blodgett films of cadmium salts of fatty acids,<sup>7,8</sup> covalent attachment to self-assembled monolayers,<sup>9,10</sup> electrostatic immobilization near charged surfactant monolayers,<sup>11</sup> diffusion into thermally evaporated fatty lipid films,<sup>12</sup> self-assembly using biotin–streptavidin connectors<sup>13</sup> and superlattice formation on self-assembled bacterial S-layers.<sup>14</sup>

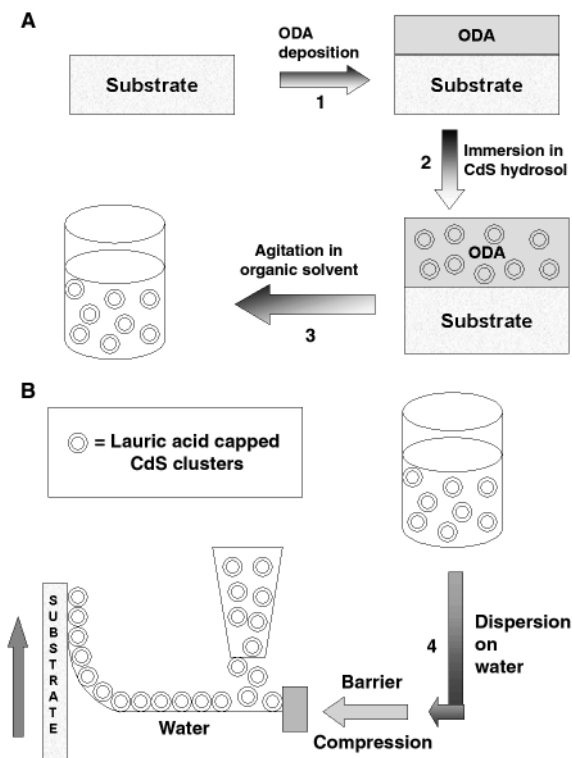
The air–water interface is an excellent medium for the organization of inorganic cations using charged amphiphilic monolayers (Langmuir monolayers)<sup>15</sup> and has now been extended to the organization of large inorganic ions,<sup>16,17</sup> colloidal nanoparticles<sup>18–21</sup> and biological macromolecules as well.<sup>22,23</sup> Fendler and co-workers have demonstrated that surface-modified “hydrophobic” nanoparticles may also be organized at the air–water interface—more specifically, *on the surface of water*—and that multilayer films of the nanoparticles can be formed on suitable substrates by the versatile Langmuir–Blodgett (LB) technique.<sup>24</sup> This approach has been used with success in the organization of polymer-capped platinum colloidal particles,<sup>25</sup> alkanethiol-capped colloidal gold particles<sup>26</sup> and buckyballs.<sup>27</sup>

Surface modification of colloidal particles to render them hydrophobic is an important requirement for the organization of inorganic particles at the air–water interface *without the ordering influence of a Langmuir monolayer*. The process of hydrophobization of the colloidal particles has hitherto been carried out by synthesis of the particles in an organic medium in the presence of a hydrophobic surfactant, as first demonstrated by Brust *et al.* for alkanethiol stabilized colloidal gold particles.<sup>28</sup> In this paper, we show that CdS nanoparticles (60 Å diameter) synthesized in an aqueous medium and stabilized using bilayers of lauric acid may be rendered hydrophobic by electrostatic extraction from solution using films of oppositely charged fatty amine molecules. The methodology is illustrated in Scheme 1A and originates from a technique developed in this laboratory for the formation of composites of colloidal particles and fatty lipid thin films by an electrostatically driven diffusion mechanism.<sup>12,29–31</sup> The first stage consists of diffusion of carboxylic acid derivatized CdS nanoparticles (surface derivatization accomplished by lauric acid bilayers)<sup>20,32</sup> from the aqueous medium into thermally evaporated fatty amine thin films (octadecylamine [ $\text{CH}_3(\text{CH}_2)_{17}\text{NH}_2$ ], ODA) by immersion of the lipid film in the hydrosol (Scheme 1A, steps 1 and 2). The CdS nanoparticle diffusion into the lipid matrix is driven by attractive electrostatic interaction between the negatively charged carboxylate groups on the colloidal particle surface and positively charged amine groups in the lipid film and has been studied in detail.<sup>12,29–31</sup> Further immersion of the CdS nanoparticle film in organic solvents under mild agitation leads to dissolution of the nanoparticles in the organic phase (Scheme 1A, step 3). The hydrophobic CdS nanoparticles were then dispersed and organized on the surface of water and multilayer films formed by the LB technique (step 4, Scheme 1B). The organization of the hydrophobic CdS nanoparticles on the surface of water and the formation of superlattice films of the particles were investigated as described below.

DOI: 10.1039/a910343k

J. Mater. Chem., 2000, 10, 1389–1393 1389

This journal is © The Royal Society of Chemistry 2000



**Scheme 1** (A) Diagram showing the hydrophobization of CdS nanoparticles extracted from aqueous solution by electrostatic interaction with thermally evaporated octadecylamine films (steps 1 and 2), followed by dispersion in an organic solvent (step 3). (B) Diagram showing the organization of hydrophobized CdS nanoparticles on the surface of water and the formation of Langmuir–Blodgett films of the nanoparticles.

## Experimental details

The CdS nanoparticles were synthesized in an aqueous medium as described elsewhere.<sup>11,12</sup> The bare CdS nanoparticles were thereafter capped with lauric acid bilayers by mixing 9 ml of the CdS nanoparticle solution with 1 ml of an ethanolic solution of lauric acid (Aldrich,  $\text{CH}_3(\text{CH}_2)_{10}\text{COOH}$ ) to yield an overall capping concentration of  $10^{-3}$  M. Prior to capping with lauric acid, the pH of the solution was adjusted to 7 using dilute ammonia. This marks a deviation from our earlier approach where the CdS nanoparticles were capped with a bifunctional molecule, 4-carboxythiophenol (4-CTP).<sup>11,12</sup> The onset of optical absorption for the aqueous CdS nanoparticles was measured using a Hewlett-Packard 8542A diode array spectrophotometer operated at a resolution of 2 nm and found to be at 475 nm (Fig. 1A), which yields a particle size of *ca.* 60 Å.<sup>33</sup> The capped CdS nanoparticles were extremely stable over time, indicating stabilization *via* lauric acid bilayers (Fig. 1A).

After ascertaining the stability of the CdS nanoparticles, the particles were extracted from the aqueous medium by immersion of 1000 Å thick octadecylamine films thermally evaporated onto glass substrates into the CdS solution held at pH 7 (Scheme 1A, step 2). The pH was adjusted to 7 since, in our earlier work, we have observed maximum CdS complexation with the ODA matrix at this value.<sup>12</sup> The electrostatically controlled diffusion of carboxylic acid derivatized CdS particles into thermally evaporated ODA films has been dealt with elsewhere<sup>12</sup> and will not be addressed in this paper. A gradual change in color of the ODA films could be observed with time of immersion and after a period of immersion of *ca.* 100 hours, intense yellow coloration of the films had occurred. Thereafter, the CdS-ODA composite films were agitated in chloroform and it was observed that, along with the excess ODA molecules in the film, the lauric acid-capped CdS nanoparticles also went into the organic medium

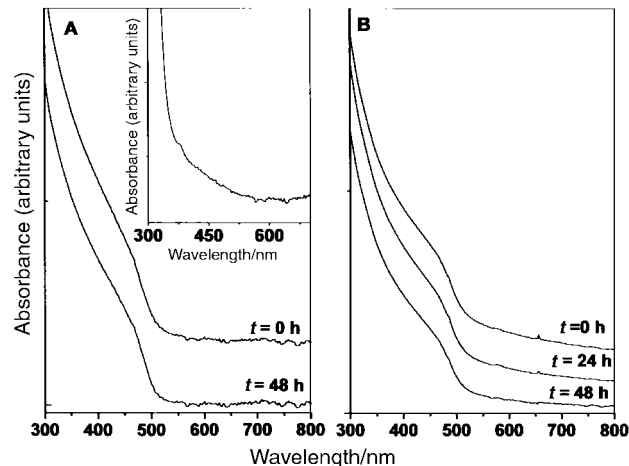


**Fig. 1** (A) UV-vis spectra recorded from CdS nanoparticles synthesized and capped with lauric acid bilayers in water as a function of time of capping. The time intervals are indicated next to the respective curves. The inset shows the UV-vis spectrum recorded from a 15 ML CdS nanoparticle LB film deposited on a quartz substrate (see text for details). (B) UV-vis spectra recorded from hydrophobized CdS nanoparticles in chloroform as a function of time of preparation of the organic solution (see text for details). The times of measurement are indicated next to the respective curves.

(Scheme 1A, step 3). The solvent was evaporated and the resulting powder washed repeatedly with absolute ethanol to rid the powder of uncoordinated ODA molecules. The lauric acid-capped CdS particles in the powder could be repeatedly dissolved in different organic solvents, indicating efficient hydrophobization of the CdS nanoparticles by this procedure. The stability of the CdS nanoparticles in organic solution was checked by UV-vis spectroscopy (Fig. 1B). A carefully washed and weighed quantity of the lauric acid-capped CdS nanoparticle powder was dissolved in chloroform and spread on the surface of water (pH 6.5), as illustrated in Scheme 1, step 4. The resulting monolayer of hydrophobized CdS nanoparticles was organized by compression in a Nima 611 Langmuir–Blodgett trough equipped with a Wilhelmy plate for surface pressure sensing. Assuming an area per lauric acid molecule of  $22 \text{ \AA}^2$  on the CdS nanoparticle surface, the weight of one  $60 \text{ \AA}$  CdS nanoparticle with the hydrophobic sheath is calculated to be  $6.67 \times 10^{-10} \text{ ng}$ . The area occupied by the CdS nanoparticle monolayer was transformed to an effective area per particle from knowledge of the concentration of the CdS nanoparticle–chloroform solution and the amount of this solution spread on the surface of water in the Langmuir–Blodgett trough. Pressure–area ( $\pi$ – $A$ ) isotherms of the nanoparticle monolayer were recorded at room temperature 30 minutes after spreading the nanoparticle solution and thereafter at different time intervals to test the stability of the nanoparticle monolayer.

After measurement of the  $\pi$ - $A$  isotherms, multilayer films of the CdS nanoparticles of different thicknesses were formed by the Langmuir–Blodgett technique<sup>15</sup> at a surface pressure of 40 dyn cm<sup>-1</sup> on quartz slides, Si(111) wafers and gold-coated AT-cut quartz crystals for UV-vis, Fourier transform infrared spectroscopy (FTIR) and quartz crystal microbalance (QCM) measurements, respectively. For the LB films grown on different substrates, monolayer transfer was observed both during the upward and downward strokes of the substrate at close to unity transfer ratio. Contact angle measurements of a sessile water drop (1  $\mu$ l) were also carried out on the CdS nanoparticle multilayer films deposited on quartz substrates using a Rame Hart 100 goniometer. The frequency counter used for the QCM studies was an Edwards FTM5 instrument operating at a frequency stability and resolution of  $\pm$ 1 Hz. For the 6 MHz crystal used in this investigation, this translates into a mass resolution of 12 ng cm<sup>-2</sup>. The frequency changes were

converted to mass loading using the standard Sauerbrey formula.<sup>34</sup> FTIR measurements of the CdS nanoparticle LB films were carried out in the diffuse reflectance mode at a resolution of  $4\text{ cm}^{-1}$  on a Shimadzu FTIR-8201 PC instrument.

## Results and discussion

The first step in this study was the carboxylic acid derivatization of CdS nanoparticles using lauric acid bilayers as briefly described in the experimental section. We have previously shown that interdigitated bilayer structures of lauric acid form on colloidal silver surfaces in an aqueous medium, that this process leads to carboxylic acid derivatization of the colloidal particle surface and consequently, electrostatic stabilization of the particles.<sup>20</sup> Such an approach has been used for the stabilization of magnetic nanoparticles as well.<sup>32</sup> It is well known that carboxylic acids readily form salts with Cd ions<sup>35</sup> and it is conceivable that lauric acid molecules would be strongly bound to the surface of CdS nanoparticles. The concentration of lauric acid taken for capping the CdS particles is much in excess of that required for forming a close-packed monolayer (*ca.*  $5 \times 10^{-5}\text{ M}$ ) on the particles. The excess lauric acid molecules would thus form an interdigitated secondary monolayer as argued in our earlier report,<sup>20</sup> thereby leading to carboxylic acid derivatization of the CdS nanoparticle surface. At pH 7, the carboxylic acid groups on the nanoparticle surface would be fully ionized and lead to stabilization of the nanoparticle solution. That this indeed is happening is indicated by the UV-vis spectra of lauric acid-capped CdS nanoparticles in an aqueous medium, which are shown in Fig. 1A. The spectra have been recorded at different time intervals of capping the nanoparticles. It is observed that the spectra recorded at  $t=0$  hours and  $t=48$  hours are almost identical with the onset of absorption occurring at the same wavelength (*ca.* 475 nm). Thus, the lauric acid molecules electrostatically stabilize the CdS particles in solution, which otherwise precipitate out of solution within a couple of hours of synthesis. Another test for carboxylic acid derivatization of the CdS nanoparticle surface is electrostatic complexation of the nanoparticles with ionized fatty lipid molecules. Thermally evaporated 1000 Å thick arachidic acid and ODA films on glass were immersed in the lauric acid-capped CdS solution for 100 hours and the UV-vis spectra recorded from the films after careful washing of the films in water and drying in flowing  $\text{N}_2$ . While an intense yellow color was observed from the ODA film, no trace of optical absorption could be seen from the AA film in the range 200–600 nm. This clearly indicates that the CdS surface is covered with carboxylic acid groups which electrostatically complex with the amine groups in the ODA film. We have previously used this strategy of surface derivatization using interdigitated bilayers with success in the surface modification of silver nanoparticles and, thereafter, in the formation of composites with fatty lipid films.<sup>30</sup>

After extraction of the lauric acid-capped CdS nanoparticles into the ODA films (step 2, Scheme 1), the nanoparticles can be dispersed in organic solvents by simple agitation of the nanocomposite films in the solvent. Hydrophobization of the CdS nanoparticles is indicated, but the exact mechanism is not immediately evident. We believe that solvation of the interdigitated regions of the hydrocarbon chains by the organic solvent molecules leads to dissolution of the lauric acid molecules in the secondary monolayer (see ref. 20 and 32 for nomenclature used) which are electrostatically complexed with ODA molecules from the lipid matrix. The end result is CdS nanoparticles capped with a strongly bound monolayer of lauric acid molecules and it is clear that such particles would be hydrophobic and soluble in the organic phase, as observed. As mentioned in the experimental section, excess ODA and lauric

acid molecules were washed away and the resulting powder dispersed in chloroform. The UV-vis spectra of the hydrophobized CdS nanoparticles in chloroform were measured at different time intervals after preparation of the solution and are shown in Fig. 1B. As in the case of the carboxylic acid derivatized CdS nanoparticles in the aqueous medium (Fig. 1A), the hydrophobic CdS particles in chloroform are also extremely stable with negligible difference in the UV-vis spectra with time. We note that organic solutions of the CdS nanoparticles are stable for many months.

An accurately weighed powder of the hydrophobized CdS nanoparticles was dissolved in chloroform and a known volume of the solution was dispersed on water (step 4, Scheme 1B). Fig. 2 shows the  $\pi$ - $A$  isotherms recorded at different times from spreading the CdS nanoparticle monolayer, the area of the monolayer having been converted to an effective area per nanoparticle as described in the experimental section. The arrows in the isotherms indicate the compression and expansion cycles of the monolayer. It is observed that hysteresis in the compression and expansion cycles is reduced as the monolayer is cycled through the  $\pi$ - $A$  isotherms and also that the area of takeoff settles into a steady value of *ca.* 37 500 Å<sup>2</sup> after *ca.* 30 minutes of spreading the monolayer (Fig. 2). At this area, the surface pressure builds up and rises steeply to around 17 000 Å<sup>2</sup> per nanoparticle, below which collapse of the monolayer occurs. If one assumes the projected dimensions of the CdS nanoparticles to be the sum of the CdS “core” (30 Å radius) and the length of the lauric acid molecule (*ca.* 17.5 Å), the area per nanoparticle at which overlap of the hydrocarbon chains between neighboring particles would occur can be shown to be *ca.* 7100 Å<sup>2</sup>. Thus, in the case of lauric acid stabilized CdS nanoparticle monolayers, surface-pressure build-up occurs at an area larger by nearly a factor of 5 than that expected from purely steric considerations. This indicates the presence of long-range repulsive interactions between the particles, possibly electrostatic in nature. However, further experiments are required before this point is clarified. The main emphasis of this paper is to demonstrate the formation of multilayer films of hydrophobic CdS nanoparticles by the LB technique.

From the  $\pi$ - $A$  isotherm measurements, a region of large incompressibility is seen to occur up to surface pressures of *ca.* 40 dyn cm<sup>-1</sup> and, therefore, multilayer LB films were transferred onto different substrates at this pressure. We would like to point out that, at this pressure, the area per CdS nanoparticle is roughly 26 000 Å<sup>2</sup>. Fig. 3 shows a plot of the

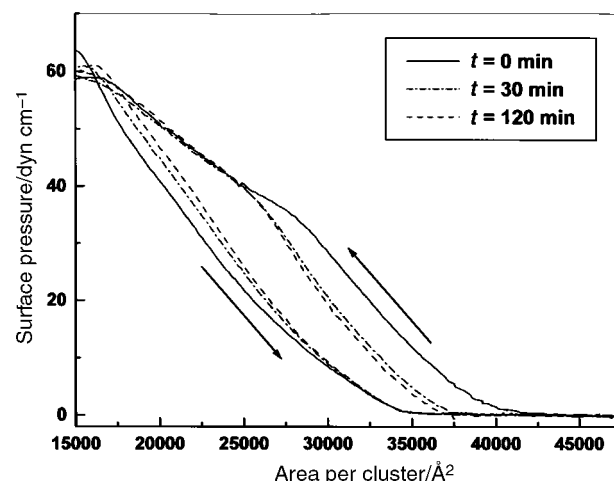


**Fig. 2**  $\pi$ - $A$  isotherms recorded from the hydrophobized CdS nanoparticle Langmuir monolayer as a function of time of spreading the monolayer. The compression and expansion cycles are indicated by arrows and the curves corresponding to different times of measurement are listed in the inset.

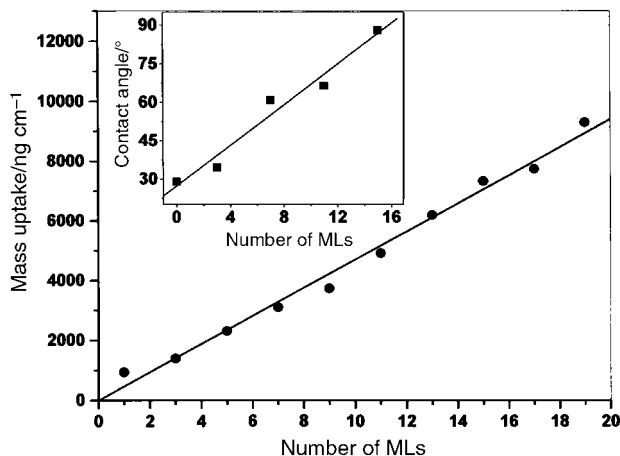


**Fig. 3** QCM mass uptake data plotted as a function of number of monolayers of the CdS nanoparticles transferred on to the quartz crystal. The solid line is a non-linear least squares fit to the QCM data. The inset shows contact angle measurements of a sessile water drop on CdS nanoparticle LB films plotted as a function of number of monolayers of the nanoparticles in the film. The solid line is to aid the eye.

QCM mass uptake *versus* the number of CdS nanoparticle monolayers (MLs) transferred onto gold-coated AT-cut quartz crystals. It can be seen from the QCM data that the mass uptake per monolayer is quite constant and independent of the substrate immersion cycle. This indicates that the CdS nanoparticle monolayer is transferred onto the substrate without significant variation in nanoparticle density up to fairly large thicknesses of the built-up LB film. The solid line is a non-linear least squares fit to the QCM data and yields a slope of *ca.* 470 ng cm<sup>-2</sup> per monolayer. As mentioned previously, the CdS nanoparticle Langmuir monolayer transfer ratio was observed to be close to unity both during the upward and downward excursions of the substrate. From the mass per CdS nanoparticle of  $6.67 \times 10^{-10}$  ng and the QCM results presented above, the area per CdS nanoparticle in the LB film is calculated to be 14 200 Å<sup>2</sup>. This value is less than that estimated from the  $\pi$ -*A* isotherm measurements and the 40 dyn cm<sup>-1</sup> nanoparticle monolayer transfer pressure (*ca.* 26 000 Å<sup>2</sup>). This discrepancy may be due to the surface roughness of the QCM quartz crystal which has not been corrected for in this study. The surface roughness factor is difficult to quantify and would lead to an overestimation of the mass uptake of the CdS nanoparticle LB films. Allowing for a roughness factor correction to the above-mentioned discrepancy, the QCM results do show that the CdS nanoparticle monolayers are transferred in a layer-by-layer fashion by the LB technique without significant variation in the nanoparticle packing density in the different layers.

Contact angles of a sessile water drop on LB films of the CdS nanoparticles of different thicknesses were measured and are shown in the inset of Fig. 3. The contact angle varies from 38° for the 3 ML (2 dips) film to 90° for the 15 ML film. While the nanoparticle films do become more hydrophobic with increasing thickness, it is interesting to note that the monolayers are fairly hydrophilic in the thickness regime studied. This may be due to the polar carboxylic acid groups in contact with the CdS particle surface within the hydrophobic sheath surrounding the particles and may explain the fairly high surface pressures observed in the  $\pi$ -*A* isotherms of the nanoparticles. In this sense, the nanoparticles may be thought of as behaving like amphiphilic molecules where the polar groups anchor the molecules to the surface of water and the hydrophobic alkyl tails give rise to the surface pressure on compression.<sup>15</sup> Also to be considered is the fact that the surface coverage of the nanoparticles per monolayer is only *ca.* 50% and this could also

explain the gradual increase in hydrophobicity of the LB films with increasing film thickness.

UV-vis spectra were recorded from LB films of the CdS nanoparticles transferred onto quartz substrates as a function of number of monolayers transferred and the spectrum recorded from a 15 ML film is shown in the inset of Fig. 1A. It is clear from the figure that effective CdS multilayers have formed and, furthermore, the onset of absorption for the LB film (*ca.* 470 nm) is in good agreement with the value obtained for the CdS nanoparticles dispersed in water (Fig. 1A) and chloroform (Fig. 1B).

FTIR spectra of a 15 ML CdS nanoparticle film grown on Si(111) wafers were recorded and the spectra obtained in the regions 3100–2700 cm<sup>-1</sup> and 1700–1400 cm<sup>-1</sup> are plotted in Fig. 4A and B, respectively. The methylene antisymmetric and symmetric vibrational modes at 2920 and 2850 cm<sup>-1</sup> are clearly seen in Fig. 4A and indicate that the hydrocarbon chains capping the CdS nanoparticles are fairly closely packed and without a significant density of defects.<sup>36</sup> In the lower frequency spectral region, a number of features are observed and have been highlighted in Fig. 4B. The bands at 1540 and 1514 cm<sup>-1</sup> are the carboxylate asymmetric stretch modes and this, in conjunction with the absence of carbonyl stretch mode at 1699 cm<sup>-1</sup>, clearly indicates not only the presence of lauric acid molecules on the CdS nanoparticle surface, but also that the lauric acid molecules are strongly bound to the particle, presumably in the form of a cadmium salt.<sup>37</sup> The feature at 1463 cm<sup>-1</sup> arises due to the methylene scissoring modes of vibration, the splitting of which is a sensitive indicator of the crystalline packing of the hydrocarbon chains.<sup>38</sup> The fact that this feature is broad without discernible splitting indicates that the chains, though close-packed (Fig. 4A and discussion earlier), are not in a crystalline environment. This is likely to be a consequence of the surface curvature of the CdS nanoparticles. Another feature at 1645 cm<sup>-1</sup> is observed and, at this stage, we are unable to interpret this peak. This has been observed in other LB films of metal salts of fatty lipids.<sup>39</sup>

In conclusion, it has been demonstrated that CdS nanoparticles derivatized with carboxylic acid groups using lauric acid bilayers may be electrostatically extracted from an aqueous medium into thermally evaporated ODA thin films and thereby rendered hydrophobic. The hydrophobization of the particles is accomplished by a monolayer of lauric acid molecules strongly co-ordinated to the CdS surface, presumably through a cadmium–lauric acid salt linkage. The hydrophobized CdS nanoparticles may be dissolved in different organic solvents

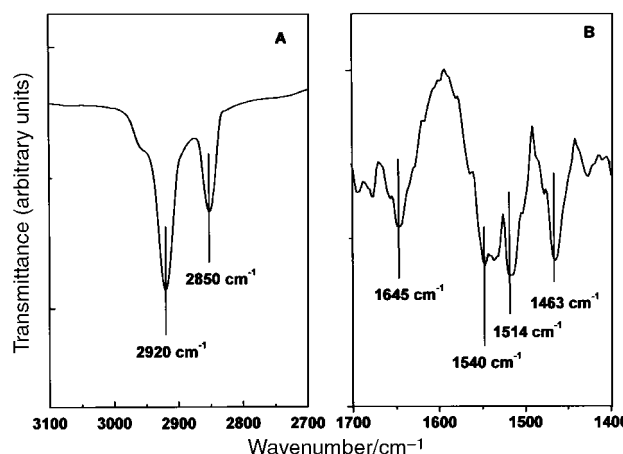


**Fig. 4** (A) FTIR spectra recorded from a 15 ML CdS nanoparticle LB film deposited on a Si(111) substrate in the range 3100–2700 cm<sup>-1</sup>. The methylene antisymmetric and symmetric vibrational modes are indicated. (B) FTIR spectra recorded from a 15 ML CdS nanoparticle LB film deposited on a Si(111) substrate in the range 1700–1400 cm<sup>-1</sup>. A number of features are identified in the figure and discussed in the text.

and organized on the surface of water to yield fairly closely packed nanoparticle Langmuir monolayers. Good quality multilayer LB films of the CdS nanoparticles can be grown on different substrates in a lamellar fashion without significant variation in the particle density. This approach for the hydrophobization of nanoparticles may be extended to control the inter-particle separation in the nanoparticle films organized at the air–water interface by altering the chain length of the surfactant molecules on the nanoparticle surface.

## Acknowledgements

A. G. thanks the Council of Scientific and Industrial Research (CSIR, Government of India) for financial assistance. This work was funded by a special grant to M. S. from the CSIR.

## References

- 1 H. Weller, *Angew. Chem., Int. Ed. Engl.*, 1993, **32**, 41.
- 2 Y. Wang and N. Herron, *J. Phys. Chem.*, 1991, **95**, 525.
- 3 V. L. Colvin, M. N. Schlamp and A. P. Alivisatos, *Nature*, 1994, **370**, 354.
- 4 N. N. Ledentsov, J. Bohrer, D. Bimberg, S. V. Zaitsev, V. M. Ustinov, A. Yu. Egorov, A. E. Zhukov, M. V. Maximov, P. S. Kopev, Zh. I. Alferov, A. O. Kosogov, U. Goesele and S. S. Ruminov, in *Proceedings of the Spring Meeting of the Materials Research Society, San Francisco, CA, 8–12 April, 1996*, ed. K. N. Tu, MRS, Pittsburgh, PA, 1996, vol. 247.
- 5 A. P. Alivisatos, *Science*, 1996, **271**, 933.
- 6 J. Yang, F. C. Meldrum and J. H. Fendler, *J. Phys. Chem.*, 1995, **99**, 5500.
- 7 R. S. Urquhart, D. N. Furlong, H. Mansur, F. Grieser, K. Tanaka and Y. Okahata, *Langmuir*, 1994, **10**, 899.
- 8 Z. Pan, J. Liu, X. Peng, T. Li, Z. Wu and M. Zhu, *Langmuir*, 1996, **12**, 851.
- 9 V. L. Colvin, A. N. Goldstein and A. P. Alivisatos, *J. Am. Chem. Soc.*, 1992, **114**, 5221.
- 10 S. Drouard, S. G. Hickey and D. J. Riley, *Chem. Commun.*, 1999, 67.
- 11 K. S. Mayya, V. Patil, P. M. Kumar and M. Sastry, *Thin Solid Films*, 1998, **312**, 300.
- 12 V. Patil and M. Sastry, *J. Chem. Soc., Faraday Trans.*, 1997, **93**, 4347.
- 13 M. Li, K. K. W. Wong and S. Mann, *Chem. Mater.*, 1999, **11**, 23.
- 14 W. Shenton, D. Pum, U. B. Sleytr and S. Mann, *Nature*, 1997, **389**, 585.
- 15 A. Ulman, *An Introduction to Ultrathin Organic Films: From Langmuir–Blodgett to Self-Assembly*, Academic Press, San Diego, CA, 1991.
- 16 P. Ganguly, D. V. Paranjape and M. Sastry, *J. Am. Chem. Soc.*, 1993, **115**, 793.
- 17 M. Clemente-Leon, C. Mingotaud, B. Agricole, C. J. Gomez-Garcia, E. Coronado and P. Delhaes, *Angew. Chem., Int. Ed. Engl.*, 1997, **36**, 1114.
- 18 M. Sastry, K. S. Mayya, V. Patil, D. V. Paranjape and S. G. Hegde, *J. Phys. Chem. B*, 1997, **101**, 4954.
- 19 K. S. Mayya, V. Patil and M. Sastry, *J. Chem. Soc., Faraday Trans.*, 1997, **93**, 3377.
- 20 V. Patil, K. S. Mayya, S. D. Pradhan and M. Sastry, *J. Am. Chem. Soc.*, 1997, **119**, 9281.
- 21 M. Sastry, K. S. Mayya and V. Patil, *Langmuir*, 1998, **14**, 5198.
- 22 A. Riccio, M. Lanzi, F. Antolini, C. De Nitti, C. Tavani and C. Nicolini, *Langmuir*, 1996, **12**, 1545.
- 23 R. Vijayalakshmi, A. Dhathathreyan, M. Kanthimathi, U. Subramanian, B. N. Nair and T. Ramasami, *Langmuir*, 1999, **15**, 2898.
- 24 J. H. Fendler and F. Meldrum, *Adv. Mater.*, 1995, **7**, 607; and references therein.
- 25 M. Sastry, V. Patil, K. S. Mayya, D. V. Paranjape, P. Singh and S. R. Sainkar, *Thin Solid Films*, 1998, **324**, 239.
- 26 J. R. Heath, C. M. Knobler and D. V. Leff, *J. Phys. Chem. B*, 1997, **101**, 189.
- 27 P. Ganguly, D. V. Paranjape, K. R. Patil, S. K. Chaudhari and S. T. Kshirsagar, *Indian J. Chem. A*, 1992, **31**, F42.
- 28 M. Brust, M. Walker, D. Bethell, D. J. Schiffrin and R. Whyman, *J. Chem. Soc., Chem. Commun.*, 1994, 801.
- 29 M. Sastry, V. Patil and K. S. Mayya, *Langmuir*, 1997, **13**, 4490.
- 30 V. Patil and M. Sastry, *Langmuir*, 1998, **14**, 2707.
- 31 V. Patil, R. B. Malvankar and M. Sastry, *Langmuir*, 1999, **15**, 8197.
- 32 L. Shen, P. E. Laibinis and T. A. Hatton, *Langmuir*, 1999, **15**, 447.
- 33 A. Henglein, *Chem. Rev.*, 1989, **89**, 1861.
- 34 G. Sauerbrey, *Z. Phys. (Munich)*, 1959, **155**, 206.
- 35 M. Linden and J. B. Rosenholm, *Langmuir*, 1995, **11**, 4499.
- 36 M. J. Hostettler, J. J. Stokes and R. W. Murray, *Langmuir*, 1996, **12**, 3604.
- 37 J. F. Rabolt, F. C. Burns, N. E. Schlotter and J. D. Swalen, *J. Chem. Phys.*, 1983, **78**, 946.
- 38 R. G. Snyder, *J. Mol. Spectrosc.*, 1961, **7**, 116.
- 39 S. Choudhury, Ph.D. thesis, University of Poona, 1996.